

Semivariogram Models Based on Geometric Offsets¹

Michael J. Pyrcz² and Clayton V. Deutsch³

Kriging-based geostatistical models require a semivariogram model. Next to the initial decision of stationarity, the choice of an appropriate variogram model is the most important decision in a geostatistical study. Common practice consists of fitting experimental semivariograms with a nested combination of proven models such as the spherical, exponential, and Gaussian models. These models work well in most cases; however, there are some shapes found in practice that are difficult to fit. We introduce a family of semivariogram models that are based on geometric shapes, analogous to the spherical semivariogram, that are known to be conditional negative definite and provide additional flexibility to fit semivariograms encountered in practice. A methodology to calculate the associated geometric shapes to match semivariograms defined in any number of directions is presented. Greater flexibility is available through the application of these geometric semivariogram models.

KEY WORDS: nested structures, kriging, stochastic simulation, geostatistics.

INTRODUCTION

Kriging-based geostatistics is routinely used for estimation and simulation of continuous and categorical geologic properties. The random function paradigm of geostatistics involves three main steps: (1) definition of the variable and the stationary domain for the variable $\{Z(\mathbf{u}), \mathbf{u} \in A\}$, which involves the definition of rock types/facies and large scale trends, (2) establish a semivariogram model for the variable, $\gamma(\mathbf{h})$, that is valid for all distances and directions found in the domain A, and (3) make inferences with kriging and Monte Carlo simulation. The reasonableness of the inferences depends on the first two steps (Pyrcz and others, in press). The expert site-specific decision of a stationary domain is arguably the most important; however, the calculation and fitting of a semivariogram model is also very important. The inference step is largely automatic once the first two

¹Received 22 March 2005; accepted 15 September 2005.

²Quantitative Stratigraphy, Earth Science R&D, Chevron Energy Technology Company, Houston, TX 77002; e-mail: mjpgy@chevron.com

³Department of Civil and Environmental Engineering, University of Alberta, Edmonton, AB, T6G 2W2 Canada; e-mail: cdeutsch@ualberta.ca

29 steps are taken. This paper is aimed at the second step of establishing a valid
 30 semivariogram model. The conventional method of modeling semivariograms
 31 by nested structures is reviewed. A suite of geometric semivariograms and a
 32 method for constructing new geometries that match custom continuity styles are
 33 presented. These geometric semivariogram models allow for greater flexibility in
 34 the generation of permissible semivariogram models.

35 CONVENTIONAL SEMIVARIOGRAM MODELING

36 The semivariogram characterizes spatial variability of the variable under
 37 consideration. Semivariogram models must be conditional negative definite; the
 38 covariance counterpart must be positive definite. This mathematical property en-
 39 sures that the semivariogram is a licit measure of distance and that all resulting
 40 variances will be non-negative for all possible configurations of conditioning data
 41 (Journel and Huijbregts, 1978, p. 35).

42 Experimental semivariogram points are calculated in the principal directions
 43 allowing for some distance and direction tolerance to find sufficient pairs. The
 44 experimental points are fitted with a sum of nested structures:

$$\gamma(h) = \sum_{i=0}^{\text{nst}} C_i \Gamma_i(\mathbf{h}) \quad (1)$$

45 where nst is the number of nested structures, $i = 0$ is commonly reserved for the
 46 nugget effect. The C_i values are the variance contribution of each nested structure;
 47 they must be non-negative. The $\Gamma_i(\mathbf{h})$ functions are valid semivariogram functions
 48 defined by a shape (e.g., spherical, exponential, Gaussian), rotation angles to allow
 49 the vector \mathbf{h} to be represented in the principal directions of continuity (h_1, h_2, h_3),
 50 and range parameters (a_1, a_2, a_3) to account for anisotropy. Standardized distances
 51 are calculated with the following equation:

$$h = \sqrt{\left(\frac{h_1}{a_1}\right)^2 + \left(\frac{h_2}{a_2}\right)^2 + \left(\frac{h_3}{a_3}\right)^2} \quad (2)$$

52 The standardized distance h is at the range of correlation in all directions. The
 53 standardized shape converts the scalar h to a standardized variogram value $\Gamma(\mathbf{h})$.

54 Semivariogram modeling has relied on fitting known conditional negative
 55 definite functions such as spherical, exponential, and Gaussian models. Linear
 56 combinations of the semivariogram models and products of covariance models
 57 are also valid functions (Deutsch and Journel, 1998, p. 24). While this provides
 58 a workable mechanism for modeling most semivariograms, there are some cases
 59 that do not well fit with this framework. Figure 1 shows an example structure

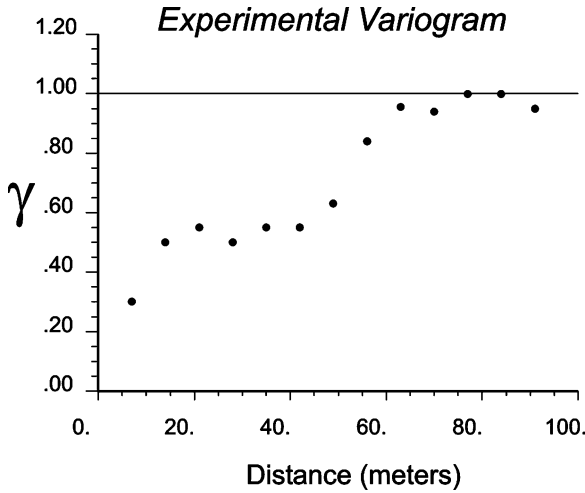


Figure 1. An example semivariogram that is not well fit by nested sets of traditional variogram models.

commonly observed in experimental semivariograms that is not easy to fit with the conventional structures. 60 61

The application of more flexible semivariogram modeling is inhibited by the difficulty in ensuring conditional negative definiteness. There is a largely unexplored suite of conditional negative definite models known as *geometric semivariograms* that provides additional flexibility. They are genetically guaranteed to be conditional negative definite and therefore avoid the burden of proof required by arbitrary semivariogram functions. 62 63 64 65 66 67

The covariance is related to the semivariogram under second-order stationarity: 68 69

$$C(\mathbf{h}) = \sigma^2 - \gamma(\mathbf{h}) \tag{3}$$

where $C(\mathbf{h})$ is the covariance and σ^2 is the variance. For ease of interpretation, semivariogram tables are shown as covariance tables since this is the common convention in kriging-based geostatistics, as covariance values provide improved stability in the solution of kriging matrices (Deutsch and Journel, 1998). 70 71 72 73

GEOMETRIC SEMIVARIOGRAMS 74

Semivariogram models based on a moving average of a generalized Poisson process are conditional negative definite (Matérn, 1960, p. 28). Geometric semivariograms result from the special case of spatial convolution where the weighting 75 76

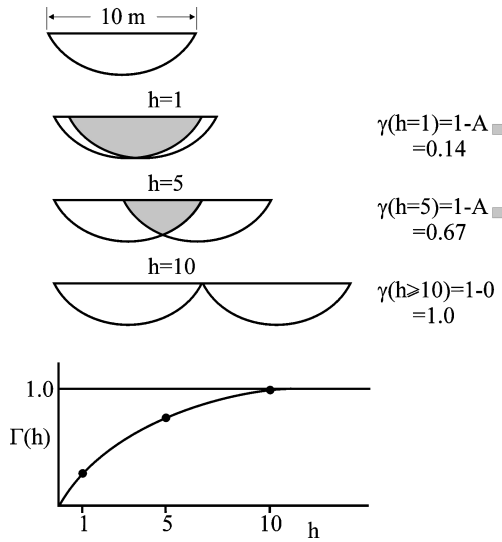


Figure 2. An example geometric object and the resulting geometric variogram in the horizontal direction. The semivariogram model is anisotropic.

77 function is reduced to a Dirac function of the form:

$$f(\mathbf{u}) = i_v(\mathbf{u}) = \begin{cases} 1, & \text{if } \mathbf{u} \in V \\ 0, & \text{if } \mathbf{u} \notin V \end{cases}$$

78

$$F(\mathbf{u}) = K_v(\mathbf{h}) = \int i_v(\mathbf{u}) \cdot i_v(\mathbf{u} + \mathbf{h}) d\mathbf{u} \tag{4}$$

79

$$\gamma(\mathbf{h}) = 1 - \frac{K_v(\mathbf{h})}{K_v(0)}$$

80 This amounts to the volume of intersection $K_v(\mathbf{h})$ of any geometric object, V , with
 81 itself offset by a lag vector, \mathbf{h} scaled by the volume of the geometric object, $K_v(0)$.
 82 Construction of a geometric semivariogram is illustrated in Figure 2.

83 A conditional negative definite model in n -D is valid in any less or equal
 84 dimensional space; for example, the spherical semivariogram, based on a 3-D
 85 geometry, is valid in three, two and one dimensions, a circular semivariogram,
 86 based on a 2-D geometry, is valid in two and one dimensions and the triangular
 87 semivariogram, based on a 1-D geometry, is valid only in one dimension.

In some cases analytical equations may be available for the volumes of intersection. Numerical integration can always be used for complicated geometric objects. The volume of intersection is calculated as:

$$\gamma(\mathbf{h}) = \underbrace{\sum_{i_z}^{n_z} \sum_{i_y}^{n_y} \sum_{i_x}^{n_x} i(\mathbf{u}_x, \mathbf{u}_y, \mathbf{u}_z)}_{K'_V(0)} - \underbrace{\sum_{i_z}^{n_z} \sum_{i_y}^{n_y} \sum_{i_x}^{n_x} i(\mathbf{u}_x, \mathbf{u}_y, \mathbf{u}_z) \cdot i(\mathbf{u}_x + \mathbf{h}_x, \mathbf{u}_y + \mathbf{h}_y, \mathbf{u}_z + \mathbf{h}_z)}_{K'_V(\mathbf{h})} \tag{5}$$

where $i(\mathbf{u}_x, \mathbf{u}_y, \mathbf{u}_z)$ and $i(\mathbf{u}_x + \mathbf{h}_x, \mathbf{u}_y + \mathbf{h}_y, \mathbf{u}_z + \mathbf{h}_z)$ are indicators set to 1 within the object and 0 outside the object and $K'_V(0)$ is the discretized volume of the geometry and $K'_V(\mathbf{h})$ is the volume of intersection given the component lag vectors $\mathbf{h}_x, \mathbf{h}_y, \mathbf{h}_z$ of lag vector \mathbf{h} . The result is a discrete covariance model for kriging or simulation. This discrete covariance model may be represented as a covariance table that may be loaded directly into kriging or a kriging-based simulation algorithm.

Limitations of Geometric Semivariogram Models

Geometric semivariogram models have some limitations in their form. (1) It is not possible to model a semivariogram above the sill variance (see Eq. (5)). This precludes the modeling of trend and hole effect continuity structures. (2) The semivariogram is linear at small lag distance. The linear feature at small lag distances prevents geometric semivariogram models from reproducing high short range continuity as seen with the Gaussian semivariogram model (Deutsch and Journel, 1998). (3) The semivariogram model is only known at discrete lag distances, unless the analytical solution is known (i.e., spherical semivariogram model). The geometry and semivariogram table are constructed to match a specific regular grid; therefore, the semivariogram may only be applied to calculate the covariance between points on this grid. These models are suitable for simulation of values on a detailed regular grid, which is increasingly common in geostatistical calculations. The data are assigned to the nearest grid node.

Some Isotropic Geometric Semivariogram Models

Isotropic geometric semivariogram models result from isotropic geometric objects. This is limited to combinations of lines (1-D), circles (2-D), spheres (3-D)

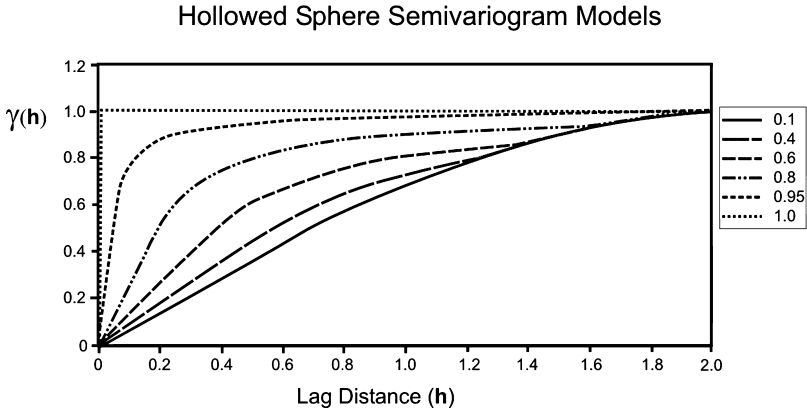


Figure 3. A series of hollowed sphere semivariogram models. The sphere radius, r_2 , is set to 1.0 and the radius of the hollowing is varied.

115 and hyperspheres (n -D, $n > 3$). These geometric models account for anisotropy by
 116 scaling the component vectors (Eq. (2)).

117 The *spherical semivariogram model* is used frequently. The spherical model
 118 is based on the standardized volume of intersection of two spheres separated by a
 119 lag vector (\mathbf{h}) as defined (Serra, 1967).

$$\gamma(\mathbf{h}) = 1 - \frac{\text{volume}(\mathbf{h})_{\text{int}}}{\text{volume}_{\text{total}}} \quad (6)$$

120 where $\text{volume}(\mathbf{h})_{\text{int}}$ is the volume of intersection and $\text{volume}_{\text{total}}$ is the total volume
 121 of the geometric object.

122 A variety of other isotropic geometric semivariogram models may be calcu-
 123 lated by hollowing of the geometric object. For example the circle in 2-D may be
 124 changed to an annular region or the sphere in 3-D may be changed to a hollow
 125 sphere. The hollow sphere results in a novel series of conditional negative definite
 126 3-D semivariogram models parameterized by the inner radius (r_1) or fraction of
 127 hollowing. A series of *hollowed spherical semivariogram* models are shown in
 128 Figure 3.

129 In the limiting cases this semivariogram is equivalent to the spherical model
 130 when r_1 equals 0.0 (the sphere is not hollowed) and approaches the nugget ef-
 131 fect as $r_1 \rightarrow r_2$. The difference between the hollowed spherical semivariogram
 132 and the spherical semivariogram is equivalent to the volume of intersection
 133 lost due to the hollowed inner sphere (Figure 4). An example hollowed sphere
 134 (fraction hollowed 0.75) geometry and resulting covariance table are shown in
 135 Figure 5.

Geometric Semivariograms

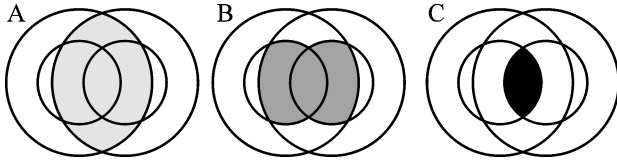


Figure 4. Volumes v_1 , v_2 , and v_3 (A, B, and C): a traditional spherical variogram model is equal to standardized v_1 subtracted from the contribution. The hollowed sphere model is equal to the spherical minus v_2 plus v_3 .

Anisotropic Geometric Semivariogram Models

136

Any geometric shape in any dimension leads to a valid semivariogram model. Slices through an approximated shape of a point bar inclined heterolithic strata (IHS) are shown on the top of Figure 6. The covariance table is calculated for this object and is shown on the bottom of Figure 6. This geometric object has resulted in a complicated anisotropic covariance table.

137
138
139
140
141

There are a variety of geologic geometries that may be applied to calculate semivariogram models. For example, characteristic geometries of architectural elements from fluvial depositional settings such as lateral accretion, downstream accretion, and channel fills (Miall, 1996, p. 93) may be suitable.

142
143
144
145

A semivariogram model constructed by an elementary geologic shape does not necessarily mean that the resulting kriged or simulated models will reproduce

146
147

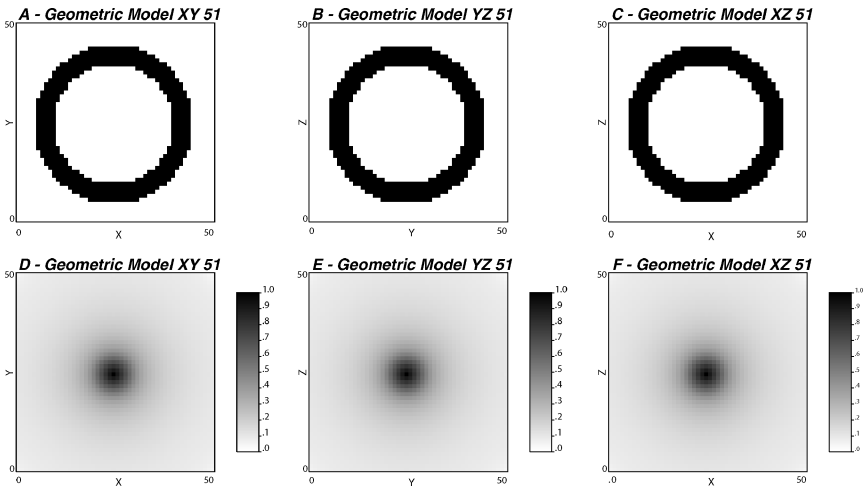


Figure 5. Center slices through the rasterized geometric object and the resulting covariance table for the hollow spherical model with a hollowed fraction of 0.75.

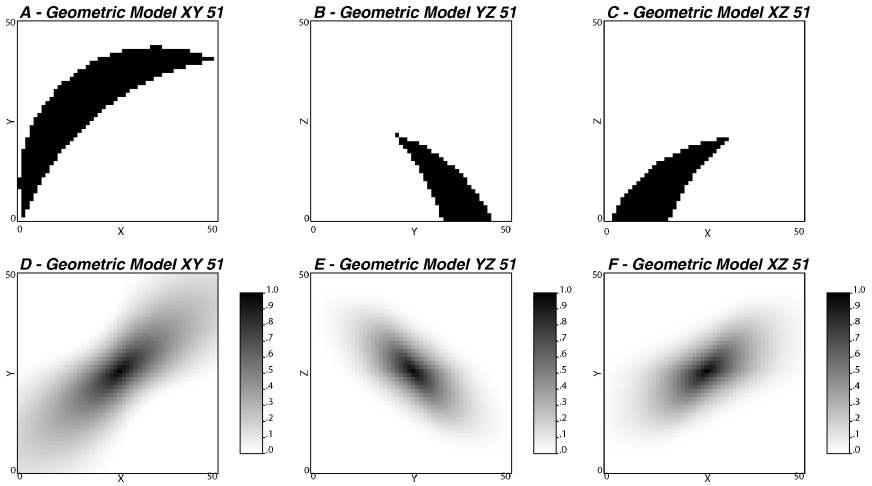


Figure 6. Center slices through the raster geometric object and the resulting covariance table for a possible IHS point bar variogram.

148 those shapes. In fact, the underlying indicator semivariogram model for spheres
 149 (of proportion $p = 1 - p_0$) embedded randomly within a matrix is related with
 150 the spherical variogram, but is not the spherical variogram:

$$\gamma(\mathbf{h}) = p_0 \left(1 - p_0^{\text{Sph}(\mathbf{h})} \right) \quad (7)$$

151 Equation (7) could be generalized to account for any geometric variogram in the
 152 exponent. Another approach would be to directly calculate the geometry that will
 153 match an experimental semivariogram model.

154 SCULPTED GEOMETRIC SEMIVARIOGRAMS

155 A method is presented to calculate the geometry to match a target semi-
 156 variogram in specified directions. An initial geometry is iteratively eroded and
 157 dilated. Changes that improve the match between the current geometric model
 158 and the target semivariograms are accepted. The resulting geometry may be ap-
 159 plied to calculate covariance tables for kriging and simulation.

160 The Inputs

161 Custom geometric semivariograms may be constructed to match continu-
 162 ity structures defined in any set of directions. These continuity structures are
 163 represented as tables with the target semivariograms and associated lag distance.

The practitioner will apply site specific information and professional judgment in assigning these target directional semivariograms. It is anticipated that these models will be fit to at least the principal directions, with additional directions added to further constrain the resulting model.

The Initial Geometry

Initial geometry is coded such that the final model may not have a range greater than the longest identified range nor less than the shortest identified range. The geometry is initialized with an outer ellipsoid of diameter equal to the largest range in all specified directions and an inner ellipsoid of diameter equal to the shortest range. No location outside the outer ellipsoid is allowed to be part of the geometry. Locations inside the inner ellipsoid are not to be taken away from the geometry. The remainder of the space may be switched between 1 and 0 iteratively to improve the reproduction of the target directional semivariograms (Fig. 7). There is no analytical model of anisotropy used for off-diagonal directions, unlike the assumption of an ellipsoidal continuity in the off-diagonal directions in traditional semivariogram models (Fig. 8). Multiple sculpted geometric semivariogram models may be calculated to represent this uncertainty in the

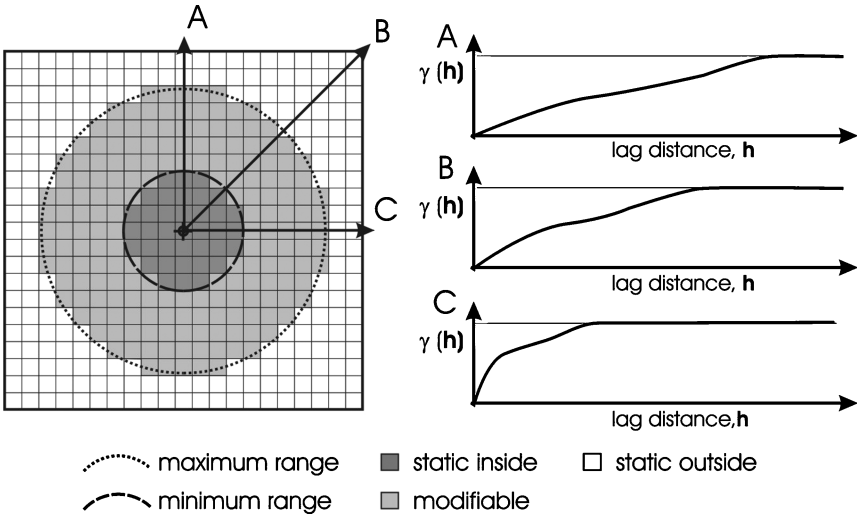


Figure 7. An initial 2-D geometry based on fit semivariograms in three directions. The area outside a circular geometry with a diameter equal to the longest identified range (direction A) is set as permanently outside the geometry. A circular geometry with a diameter equal to the shortest identified range (direction C) is set as permanently inside the geometry. The remainder may be modified iteratively to fit the semivariograms in each identified direction.

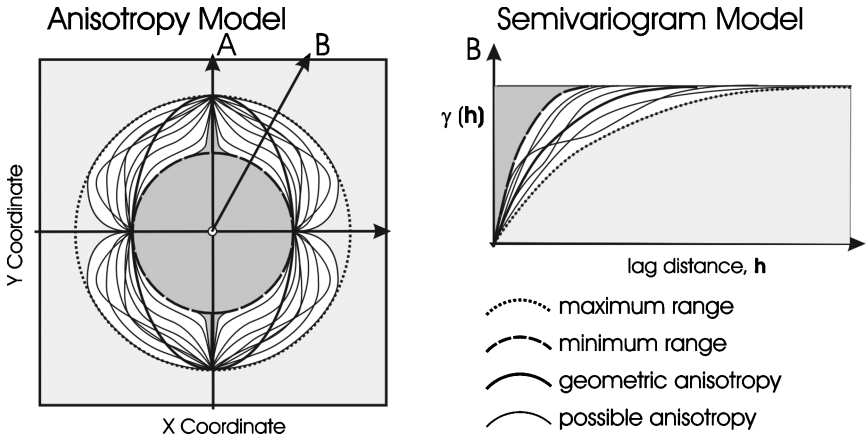


Figure 8. The constraints on sculpted geometric semivariogram models. The major and minor principal directions (directions A and B respectively) and the traditional anisotropy ellipsoid are shown. The sculpted semivariogram model is constrained such that the range in the off-diagonal directions (such as direction B) may not exceed the range in the major direction or be exceeded by the range in the minor direction. The anisotropy may be expressed in various forms within this constraint.

181 off-diagonal directions. If adequate information is available, experimental semi-
 182 variogram fits in off-diagonal directions may be integrated to further constrain the
 183 model.

184 Zonal anisotropy may be included by setting the initial diameter large relative
 185 to the size of the covariance lookup table.

186 The Iterations and Convergence Criteria

187 An objective function is applied to characterize mismatch between the target
 188 and sculpted geometric semivariogram models. This objective function is shown
 189 below:

$$O = \sum_{i=1}^{nDir} \sum_{j=1}^{nLag} |\gamma^{geo}(\mathbf{h}_{i,j}) - \gamma^t(\mathbf{h}_{i,j})| \quad (8)$$

190 where $\gamma^{geo}(\mathbf{h}_{i,j})$ and $\gamma^t(\mathbf{h}_{i,j})$ are the current geometric and target semivariogram
 191 models for each indicated direction, i , and lag, j . This objective function
 192 weights all lag distances equally. It is common practice to focus on fitting
 193 short scale structures, the addition of a weight (such as $1/\mathbf{h}_{i,j}$) would account
 194 for this.

Geometric Semivariograms

The nodes within the modifiable zone (Fig. 7) are visited in order from the outside inwards. This ordering is based on the distance function of initial geometry (Vincent and Algorithms, 1993). This amounts to the assignment of the distance to the nearest periphery of the geometry at all nodes within the geometry. The distance function is sorted in ascending order with pointer arrays permuted.

For each location, the geometry code is switched. The location within the current geometry is eroded ($i(\mathbf{u}_i) = 1 \rightarrow 0$) or outside the current geometry dilated ($i(\mathbf{u}_i) = 0 \rightarrow 1$). The objective function is updated and if the perturbation reduces the objective function it is accepted. The algorithms proceeds until either a maximum number of iterations are performed or until a specified number of iterations occur without acceptance of a perturbation.

Example Sculpted Semivariogram Models

A large suite of sculpted semivariogram models were calculated. Many unconditional 2-D simulation models were calculated with a variety of input semivariogram parameters (ranges, nugget effects, anisotropies and structure types). Then the experimental semivariograms were calculated for the 0°, 45°, 90° and 135° azimuths. These experimental semivariograms were applied as input for the construction of 2-D sculpted geometric semivariograms. The resulting covariance tables were checked for ill conditioned covariance matrices; all variances were positive (as required by theory) and all kriging weights were reasonable minus [-1, 1].

An example of 2-D sculpted geometric semivariogram model is shown in Figure 9. This example demonstrates the flexibility and some limitations of sculpted semivariogram models. Note that the trend in the input directional variograms is not reproduced since geometric models may not exceed the sill. The zonal anisotropy is not reproduced since the largest range was set to 40 units.

Another example of 2-D sculpted geometric semivariogram model is shown in Figure 10. This model represents a phenomenon with a high nugget effect and a high degree of anisotropy. Note that the nugget effect is reproduced by a lack of contiguity in the geometry and the anisotropy results in anisotropy in the geometry. Another method for incorporating the nugget effect is to model other continuity structures and then add the nugget effect to this discrete model.

SEMIVARIOGRAM MODELING PROCEDURE

The flexible semivariogram modeling is summarized. This methodology requires the following steps: (1) assess the continuity of the modeled phenomenon in at least the principal directions, (2) construct a geometric object either from characteristic geometries or by the iterative method introduced in this paper with a

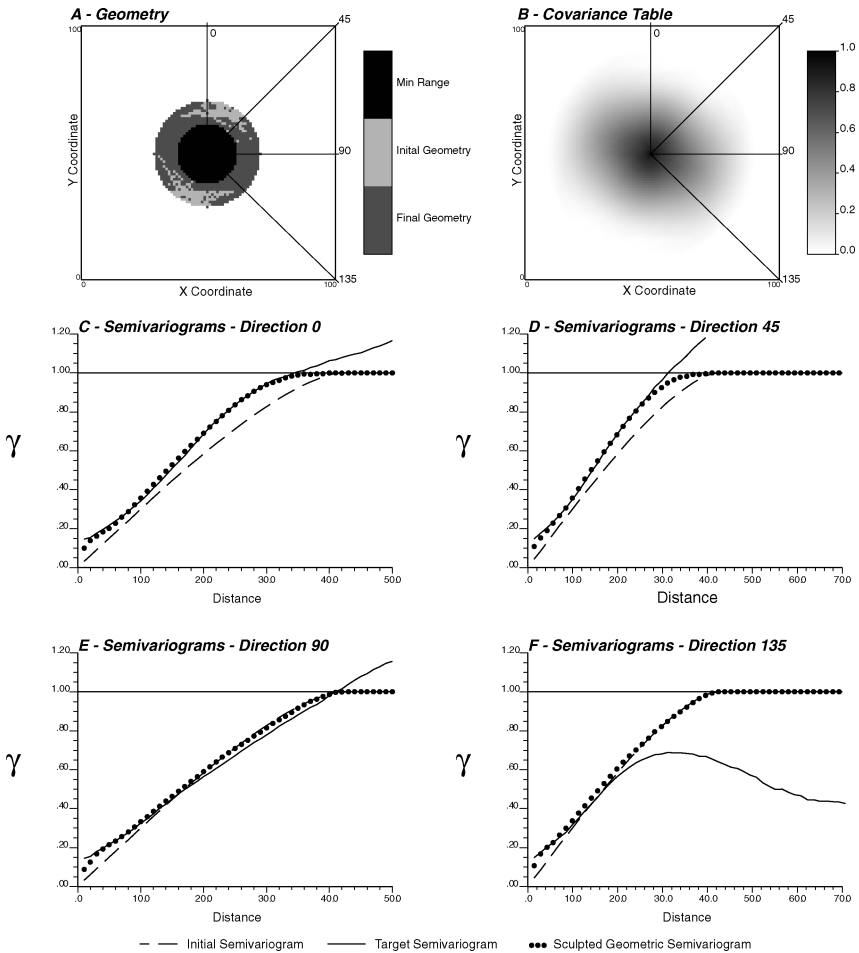


Figure 9. A 2-D geometry and covariance table for a sculpted geometric semivariogram model based on a phenomenon with high continuity. The initial geometry, the target directional models and resulting sculpted geometric semivariogram models in 0°, 45°, 90° and 135° directions are shown. The longest range of continuity was assigned as 40 units. The target models are experimental semivariograms from unconditional sequential Gaussian simulation.

232 resolution greater than or equivalent to the resolution of the model to be estimated
 233 or simulated, (3) calculate a discrete covariance table from this geometry, (4)
 234 load this covariance table into the kriging or simulation algorithm. These direc-
 235 tional models may be regression fits of the experimental semivariogram points, or
 236 even hand drawn. The key is to build models that integrate the available geologic
 237 information.

Geometric Semivariograms

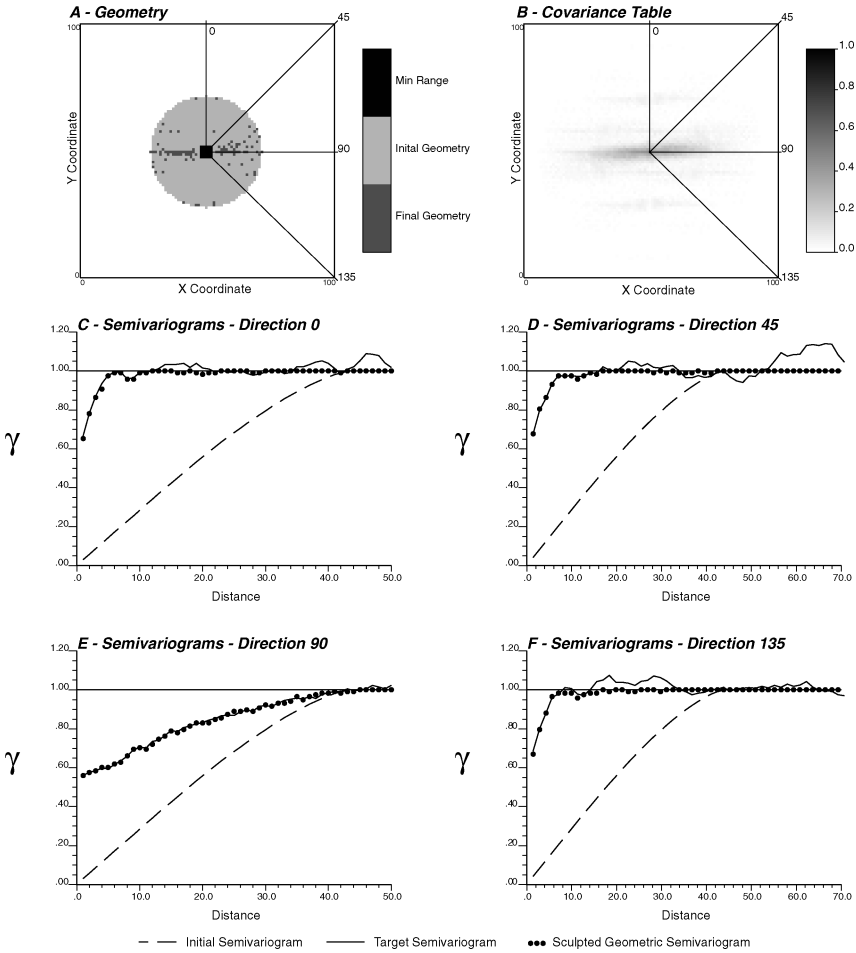


Figure 10. A 2-D geometry and covariance table for a sculpted geometric semivariogram model based on a phenomenon with high anisotropy and large nugget effect. The initial geometry, the target directional models and resulting sculpted geometric semivariogram models in 0°, 45°, 90° and 135° directions are shown. The target models are experimental semivariograms from unconditional sequential Gaussian simulation.

CONCLUSIONS

238

The choice of semivariogram model has a major affect on kriging and kriging-based simulation. These models are commonly modeled as nested combinations of proven models. Geometric semivariogram models provide a suite of conditional negative definite models for improved semivariogram modeling flexibility.

239
240
241
242

243 A flexible method has been presented for constructing geometries for geomet-
 244 ric semivariograms that reproduce spatial continuity identified in principal and
 245 additional directions.

246 The required computer code is straightforward and efficient and is available
 247 from the authors. All semivariogram models proposed here are guaranteed to be
 248 conditional negative definite; therefore, there are no issues with implementation.
 249 Flexible fitting of semivariogram models allows for greater focus on the avail-
 250 able experimental semivariogram and geologic information without the limitation
 251 imposed with the traditional method of nested structures.

252 REFERENCES

- 253 Deutsch, C. V., and Journel, A. G., 1998, *GSLIB: geostatistical software library and user's guide* 2nd
 254 ed.: Oxford University Press, New York, 369 pp.
- 255 Journel, A. G., and Huijbregts, Ch. J., 1978, *Mining geostatistics*: Academic Press, New York, 600 p.
- 256 Matérn, B., 1960, *Spatial variation*, of lecture notes in statistics 2nd edn., Vol.36: Springer, New York,
 257 First edition published by Meddelanden fran Statens Skogsforskningsinstitut, band 49, no. 5,
 258 1960, 151 p.
- 259 Miall, A. D., 1996, *The geology of fluvial deposits: sedimentary facies, basin analysis and petroleum*
 260 *geology*: Springer; Berlin, 582 p.
- 261 Pyrcz, M. J., Gringarten, E., Frykman, P., and Deutsch, C. V., in press, Representative input parameters
 262 for geostatistical simulation, *In* Coburn, T. C., ed., *Stochastic Modeling II: AAPG Computer*
 263 *Applications in Geology*, No N, Qmen. Assoc. Petrol. Geol., Tulsa.
- 264 Serra, J., 1967, Un critère nouveau de découvertes de structures: le variogramme: *Sciences de la Terre*,
 265 v. 12, p. 275–299.
- 266 Vincent, L., 1993, Morphological algorithms, *In*: Dougherty, E. R., ed., *Mathematical Morphology in*
 267 *Image Processing*, Marcel Dekker, New York, p. 255–288.

Queries to Author:

A1: Au: Please update Ref. Pycz et al.,in press.